Agriculture and Food

AIMS Agriculture and Food, 9(1): 84–107.
DOI: 10.3934/agrfood.2024006
Received: 08 October 2023
Revised: 13 December 2023
Accepted: 13 December 2023
Published: 29 December 2023

http://www.aimspress.com/journal/agriculture

Research article

Evaluation of meteorological datasets in estimating the water footprint components of wheat and maize (case study: Qazvin, Iran)

Hadi Ramezani Etedali[1,*], Faraz Gorginpaveh[2], Parisa Kakvand[3], Ahmed Elbeltagi[4], Brian Collins[5]

[1] Department of Water Sciences and Engineering, Imam Khomeini International University, Qazvin, Iran
[2] Civil and Environmental Engineering, Syracuse University, Syracuse, USA
[3] Department of Irrigation and Reclamation, University of Tehran, Karaj, Iran
[4] Agricultural Engineering Department, Faculty of Agriculture, Mansoura University, Mansoura, Egypt
[5] Centre for Sustainable Agricultural Systems, Institute for Life Sciences and the Environment, University of Southern Queensland, Toowoomba, Queensland, Australia

* **Correspondence:** Email: Ramezani@eng.ikiu.ac.ir; Tel: +982833901278; Fax: +982833901278.

Abstract: Given the critical role of precise meteorological parameter estimation in water resources management, particularly concerning the water footprint (WF) concept and considering the scarcity of data, this study utilized thirty years of data from four meteorological datasets to estimate the WF of two main cereals, wheat and maize, in Qazvin province, Iran. AquaCrop was used to calculate the WF parameters based on a synoptic station and the closest datasets to the synoptic station. Coefficient of determination (R^2), root-mean-square deviation (RMSE) and its normalization (NRMSE), and maximum error (ME) were used to compare the results. The results showed that these datasets efficiently estimate the WF components and can be used instead of synoptic stations. Also, all datasets were more efficient in estimating the green WF than the blue WF. The Global Precipitation Climatology Center (GPCC) dataset was the most efficient dataset in assessing the WF components for wheat, where the RMSE and NRMSE were 84.8 m^3/ton and 17.18%. These amounts were 55.1 m^3/ton and 12.96% for the green WF. For estimating the blue WF of maize, the Climatic Research Unit (CRU) datasets were the most efficient datasets in assessing the WF components of maize, which were 35.58 m^3/ton and 15.91%. This study demonstrated the robustness of meteorological datasets in accurately estimating the components of the WF. Furthermore, the study advocates for the utilization of diverse datasets in estimating meteorological and crop parameters, recommending this approach for different crops across various regions.

Keywords: crop growth; precipitation; multi-crop model; crop pattern; cereal

1. Introduction

According to the importance of climate variation and its effect on precipitation, temperature and agricultural yield [1], accurate estimation of meteorological parameters and monitoring the changes in the past are crucial [2]. Significantly, it will help water resources managers to plan more efficiently and conserve water resources for the next generations [3–5]. According to Worqlul et al. (2015), most places in the world are facing a considerable lack of data in the time and space scales in estimating and predicting the amount of precipitation, evapotranspiration and other meteorological and crop parameters [6], and this has always been a significant challenge to agricultural and water resources managers worldwide [7]. The number of synoptic stations and their accuracy is not always acceptable in some regions [8]. Also, these stations cannot estimate meteorological parameters in the past [9]. The accurate estimate of these parameters will help managers to use water resources and lands more efficiently, and it will be possible to estimate future changes in meteorological patterns [10].

Numerous simulation methods have been used in different ways to increase the efficiency and performance of different systems, and they cover a wide range of fields from infrastructure management to irrigation and water management [11–13]. Simulation models can estimate the water requirements of crops, yield and other crop parameters. Although there has been a range of crop simulation models reported in the literature which quantify the effects of stresses on crop growth, development and yield (e.g., DSSAT [14], CropSyst [15], APSIM [16], Hybrid-Maize [17] and CROPWAT [18]), they have several issues. The common issue of these models is their requirement for highly detailed input data and information about crop growth, which may not be available in most locations worldwide [19]. FAO developed AquaCrop in 2009 to address these limitations [20]. AquaCrop is a multi-crop model that simulates the water-limited yield for herbaceous crops under different biophysical and management conditions and provides a good balance between robustness, simplicity and output accuracy, and it can be used for a large number of crops [20,21]. Some studies include wheat [22], maize [23], barley [24] and cotton [25], as well as multi-crop analysis [26]. Also, the probabilistic behavior of this model has been studied recently [27].

By the development of satellites and using remote sensing techniques, a wide range of projects can be implemented, at local, regional, national and global scales, which are cost effective and time saving [28]. Also, they cover data in different and various periods from an hourly scale to daily, monthly and yearly scales. Furthermore, with such data, they make it possible to study changes and monitor terrestrial phenomena [29]. There has been significant research in remote sensing in various studies and study areas, such as agricultural and natural resource management [30], groundwater [31], flood [32], drought [33], climate change [34], water quality [35], fire monitoring [36], salinity management [37] and crop water requirement [38]. These studies employed different approaches and methods to enhance the efficiency of different scope-specific applications, with each study claiming a positive impact on reducing inaccuracies.

Virtual water (VW) trade is another concept, which with the WF can be useful for sustainable management of groundwater and surface water resources, especially in regions with dry and semi-dry climates [39]. The VW trade has been suggested in the literature as an approach for saving water resources and achieving water security at the regional, national and international levels [40–42]. It was

also used in Iran for different regions, such as the south [43] or east [44], or the whole country [45].

In this study, the "water footprint" (WF) concept was used as a measure of the water amount used for producing wheat and maize. Hoekstra (2003) introduced the concept of WF, which is an indicator of the use of freshwater resources in different sections of the production process, i.e., a consumption-based indicator in which consumption refers to the total amount of water used to produce a certain amount of output [46,47]. This term facilitates water resources management, especially in water-scarce areas. This concept has been adopted in numerous studies and study areas (e.g., resources [48], urban planning [49], groundwater [50], crop patterns in dry regions [51]) and for different crops (e.g., main cereals [47,52], citrus [43], rainfed wheat and maize [53,54]). This concept was also applied in regional accounting for both irrigated and rain-fed lands with the goal of increasing efficiency of agricultural utilization applications [54–57].

The present study employs a holistic approach, combining the WF concept, climate data derived from multiple datasets and crop modeling to estimate the WF of two predominant cereal crops in the Qazvin province of Iran. In this methodology, we utilize three decades of data from four distinct datasets (CRU, GPCC, AgCFSR and AgMERRA) within the AquaCrop model to calculate the WF of wheat and maize crops in this geographic area. Subsequently, the results are compared and assessed against data from the nearest synoptic stations within the province.

The overarching objectives of this research encompass two key aims. First, we endeavor to ascertain the accuracies of various datasets in estimating agricultural production within this specific land, which holds significant importance, especially for disadvantaged regions. Second, we seek to identify the dataset that best aligns with the unique characteristics of this location, enabling us to make informed choices regarding dataset selection in comparison to others for future applications.

2. Materials and methods

2.1. Study area and crops

Qazvin province, with an area of 15,821 km^2, reaches from 35° 37' N to 36° 45' N and from 48° 45' E to 50° 50' E", with an arid to semi-arid climate. It has relatively warm summers and cold winters, with 14 ℃ and 339.4 mm as its mean annual temperature and precipitation, respectively. The location of the province in the country is presented in Figure 1. The Qazvin Plain, situated withing the province, represents the largest area within the Salt Lake basin, boasting the most extensive cultivation area for diverse crops among all plains in the region. The main irrigated crops are wheat, maize, corn, alfalfa, tomato and canola. According to the Agricultural Jihad Ministry (2015), 144,000 hectares of land under cultivation is dedicated to wheat, which leads to 315,000 tons of production per year. Maize, the other important crop in the plain, produces 100,8015 tons per year, which accounts for 45% of the plain's irrigation. This crop covers 18,132 hectares of land under cultivation. As is demonstrated in Table 1, these crops are responsible for 81% of agricultural production and 90% of the irrigated lands of this plain.

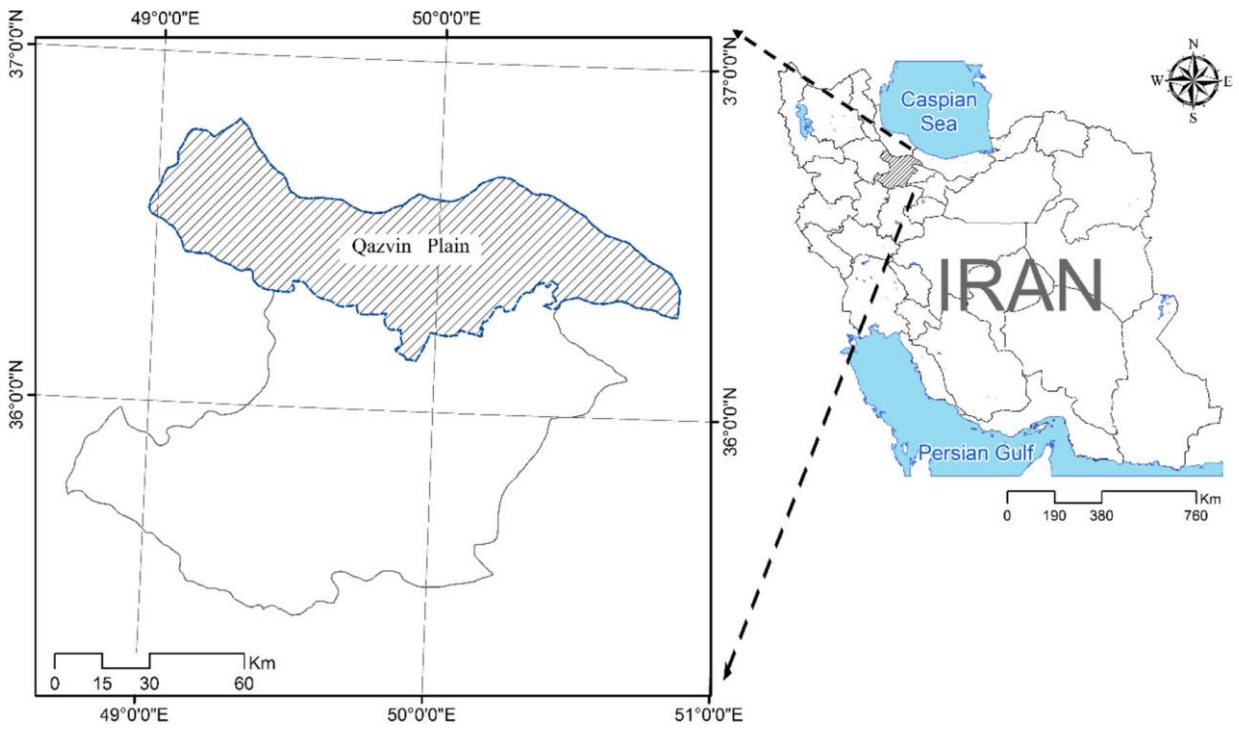

Figure 1. The location of the Qazvin Plain in Iran [61].

Table 1. Percentages of area and production of main irrigated crops in the Qazvin Plain.

Crop	Percentage of area	Percentage of production
Wheat	39	10
Barley	16	4
Maize	11	42
Alfalfa	12	9
Tomato	5	12
Canola	1	0.2
Others	10	19

In this study, the data of four meteorological datasets from the Qazvin province were gathered from meteorological datasets in two ways: the nearest neighbor point to the synoptic station (K1) and the average of the four nearest neighbor points to the synoptic station (K4). They can be reliable for climate variable estimations. Figure 2 shows the procedure of choosing the closest points to the synoptic stations in a way that the black color point is the synoptic station, and the other point is the closest point to the station in the grid made by dataset. If there is only one point, then it is called the K1 procedure; meanwhile, for four nearest points, the K4 name is assigned to this data. The four points are averaged, and then the average was used in the calculations. The grid size differs for each meteorological dataset. Then, the results of them were compared with each other to show that how much they differ in compare with each other and in compare with the synoptic station.

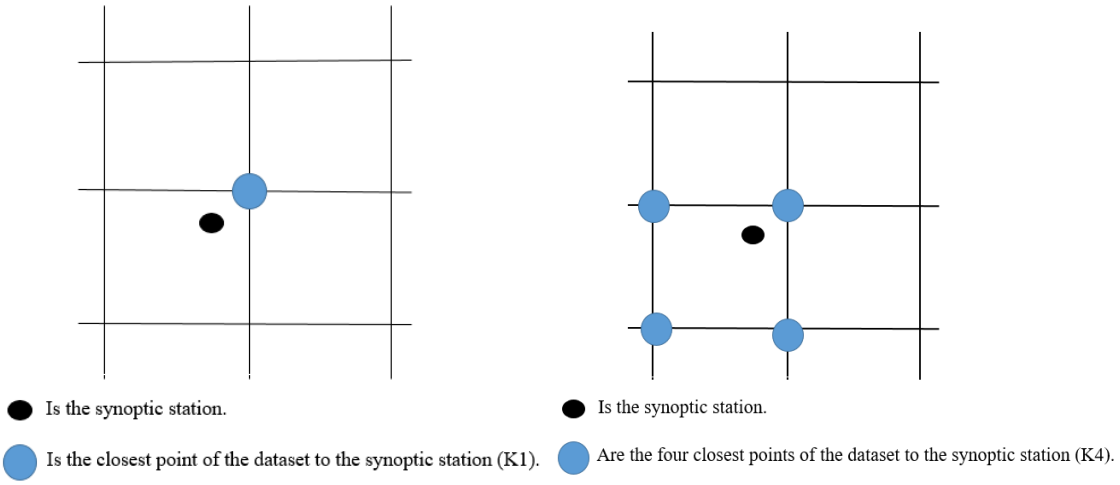

Figure 2. The location of the synoptic station and the nearest point of the dataset (K1), and the four nearest points of the dataset (K4). The mesh and the location of the synoptic station is hypothetical. The size of the mesh varies based on choosing different meteorological datasets.

2.2. Water footprint (WF)

Water footprint is a spatial and temporal measure of the total volume of freshwater that has been used for producing something. WF consists of three components, the blue WF, the green WF and the gray WF. The volume of the water used in the production of crops, known as net water requirement, is called the blue WF. It is the volume of water evaporated for the production of agricultural products. The green WF is related to the effective rainfall stored in the soil and supplies crop water demand. Gray WF refers to the volume of water that is required to dilute pollutants (industrial discharges, seepage from tailing ponds at mining operations, untreated municipal wastewater or nonpoint source pollution such as agricultural runoff or urban runoff) to such an extent that the quality of the water meets agreed water quality standards [46,62–65]. In this study, only the blue and green WF were estimated. The following equations can determine these two elements:

$$WF_{\text{Blue}} = \frac{(ET_c - P_e)\times 10}{Y} \quad (1)$$

$$WF_{Green} = \frac{P_e \times 10}{Y} \quad (2)$$

WF_{Blue} and WF_{Green} are the blue WF and the green WF, respectively, in m^3t^{-1}, P_e is the total effective rainfall during the crop-growing season (mm), ET_c is the crop evapotranspiration (mm), and Y is the crop yield (ton hectare-1) that was calculated by the AquaCrop model from the average of the 30 years of measured values in the field. In this model, the ET_c calculated by the FAO Penman-Montieth method by the AquaCrop model and c, the crop coefficient based on each crop and region, can be varied [66,67]. For this study, the initial values of the coefficient from FAO were calibrated based on the Qazvin Plain and the crops of this study in another study [68]. The water uses and the WF components of wheat and maize in the Qazvin plain are represented in Table 2. Finally, the P_e values were calculated by the United States Department of Agriculture (USDA).

Table 2. Meteorological data of Qazvin synoptic station (base period averages).

Crop	Water use (mm)		WF (m^3/ton)		
	ET_c	P_{eff}	Green	Blue	Total
Wheat	475	303	769	437	2673
Maize	695	29	882	375	2651

2.3. Dataset

In this research, the efficiencies of four datasets, CRU, GPCC, AgCFSR and AgMERRA, were evaluated. Most of these datasets have been evaluated in different countries, such as China [69], Iran [70] and Pakistan [71], which shows the high efficiency of different datasets in water and climate research. A brief explanation of each dataset is given below.

2.3.1. CRU TS

The Climatic Research Unit (CRU) Time-Series (TS) dataset, which was developed by the UK's Natural Environment Research Council (NERC) and the US Department of Energy, is one of the reliable and popular available gridded datasets. This dataset contains ten weather variables (including cloud cover, precipitation, temperature, vapor pressure, potential evapotranspiration and frost day frequency) from over 5000 individual weather stations across the planet (except Antarctica), interpolated into 0.5° × 0.5° grid cells [72]. This gridded time-series dataset covers the period 1901–2014 by months, and its coverage includes all land areas. It is based on a dense station network with good quality control and homogeneity check [73].

2.3.2. GPCC

The Global Precipitation Climatology Center (GPCC), which operates under the auspices of the World Meteorological Organization (WMO), provides global precipitation analyses for monitoring and research of the earth's climate with monthly and daily precipitation datasets. The GPCC products are available in spatial resolutions of 1.0° × 1.0°, 2.5° × 2.5° and 0.5° × 0.5°. This dataset covers data from 1901 to 2009 [74]. GPCC claims to provide the best possible observational gridded monthly land-surface precipitation data in the world, as all of its products are fed by the world's largest database of quality-controlled rain gauge data gathered from eight different sources, allowing for cross-checking of redundant data gathered from multiple sources [75].

2.3.3. AgMERRA and AgCFSR

The AgMERRA and AgCFSR climate forcing datasets, which are the third and the fourth datasets in this study, were created as an element of the Agricultural Model Intercomparison and Improvement Project (AgMIP). These two datasets provide consistent, daily time series throughout 1980–2010 focusing on crop and livestock models at the local level, regional assessment of food security and global economic impacts [76,77]. This dataset covers global variables that are required for agricultural models. The data is interpolated into 0.25° × 0.25° grids [78].

2.4. The AquaCrop Model

The AquaCrop model, version 5, which was introduced by FAO, is used in this study to compute the WF components. This model simulates yield and biomass in relation to the water available to plants that were introduced by the Doorenbos and Kassam empirical relation [79]. The model estimates the values of the water productivity index (transpiration). The crop yield in a daily time stems from separation transpiration and evaporation from evapotranspiration and the amount of biomass produced by the harvest index [25]. It also uses a green cover on the ground instead of the leaf surface index. In this model, the growth rate index does have great importance, and it examines the productivity index instead of the ratio of the relative decrease in performance. The relation between the maximum and actual yield and the maximum and the actual evapotranspiration is calculated by the following equation:

$$\left(1-\frac{Y}{Y_x}\right)=K_y\left(1-\frac{ET}{ET_x}\right) \tag{3}$$

Where Y_x and Y are the maximum and the actual yield, respectively, ET_x and ET are the maximum and actual evapotranspiration, respectively, and K_y is the ratio between the relative decrease in yield and the relative decrease in evapotranspiration.

According to Golabi and Naseri, four categories of inputs of AquaCrop are meteorological, plant, managerial and soil information [80]. Also, the AquaCrop model runs for net water requirement, and there is no water or irrigation system definition in the model. So, without any regard to the agricultural system, we provided net water requirement to the model as an input.

2.5. Statistical analysis

In this study, the estimated WF components of two crops (maize and wheat) by four datasets are evaluated by the estimation of WF components of the synoptic station in the Qazvin province. The evaluation criteria are determination coefficient (R^2), root mean square error (RMSE), normal square root mean square error (NRMSE) and the maximum error (ME). The relations between WF components to compute RMSE, NRMSE and ME are presented below.

$$RMSE=\sqrt{average\ (WF_{syn}-WF_{dataset})^2} \tag{4}$$

$$NRMSE=\frac{RMSE}{Average WF_{syn}} \tag{5}$$

$$ME=|WF_{syn}-WF_{dataset}| \tag{6}$$

3. Results

3.1. Wheat WF

3.1.1. CRU

Figure 3 shows the amounts of the blue and the green WF of wheat estimated by the synoptic station and CRU, respectively. According to these figures, the amounts of R^2 are 0.414 and 0.328 for the K1 and the K4 estimations of blue WF and 0.463 and 0.362 for the K1 and the K4 estimations of green WF. For the blue WF, the values of RMSE for the K1 and K4 estimation are 131.03 and 136.21 m^3/ton, while these values for the green WF are 94.93 and 90.59 m^3/ton. The values of the NRMSE are 26.55 and 27.6% for the blue WF and 22.32 and 21.3% for the green WF, respectively. Finally, 249.03 and 293.62 m^3/ton are the maximum errors in estimating the blue WF with K1 and K4, and 171.51 and 202.73 m^3/ton are those for the green WF, respectively. Overall, the CRU dataset tends to overestimate the amount of blue WF compared with the observational data, while it tends to underestimate the amount of green WF. For both K1 and K4, the estimations are close to each other.

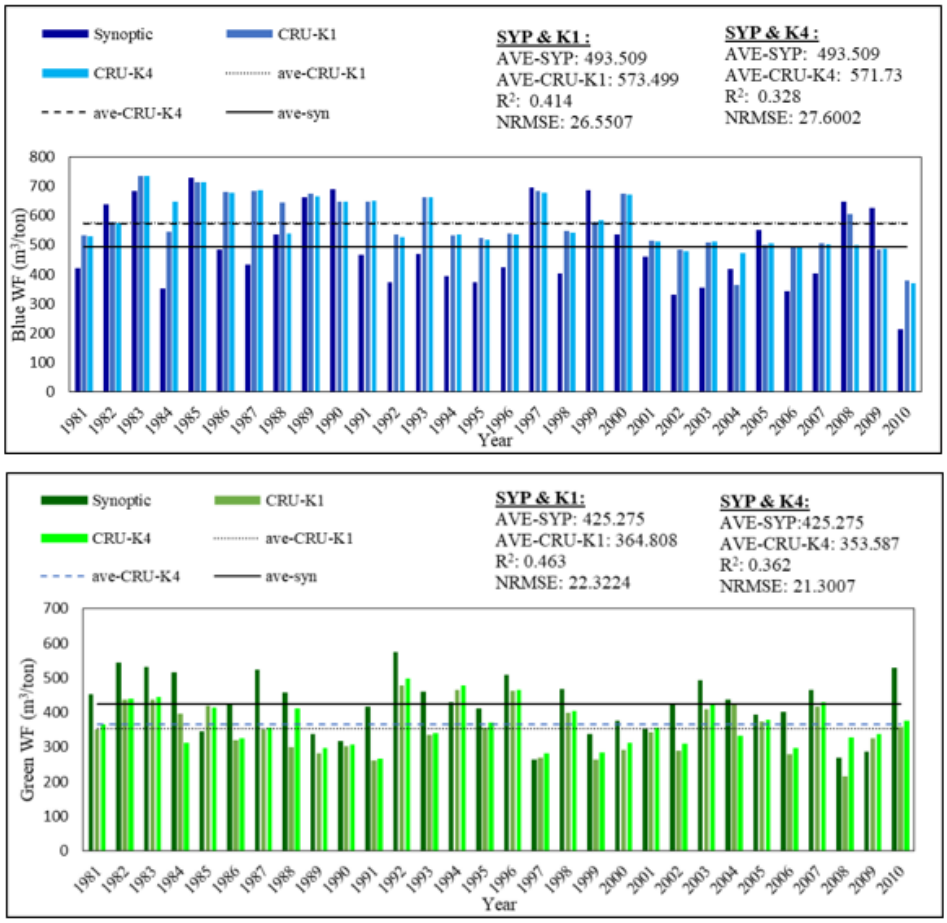

Figure 3. The amounts of the blue and green WF of wheat estimated by the synoptic station and CRU.

3.1.2. GPCC

The amounts of the blue and the green WF estimated by the synoptic station and GPCC, for both K1 and K4, are shown in Figure 4. According to the figures, the amounts of R^2, RMSE and NRMSE for the blue WF of GPCC are 0.615 and 0.537, the amounts of RMSE are 84.80 m^3/ton and 100.2 m^3/ton, and the amounts of NRMSE are 17.18 and 20.3% for K1 and K4, respectively. These amounts for the green WF are 0.601 and 0.6, 55.1 m^3/ton and 55.39 m^3/ton for K1, and 12.95% and 13.02% for K4. The ME of the K1 and K4 estimations of GPCC are 159.35 and 163.58 m^3/ton for the blue WF and 98.36 and 143.18 m^3/ton for the green WF. According to the results, both K1 and K4 are close together, but estimation with the nearest neighbor point (K1) is more efficient than the four neighbor points (K4). Although GPCC is overestimating the blue WF for K1 and K4, the amount of estimation is approximately close to the synoptic station for the green WF.

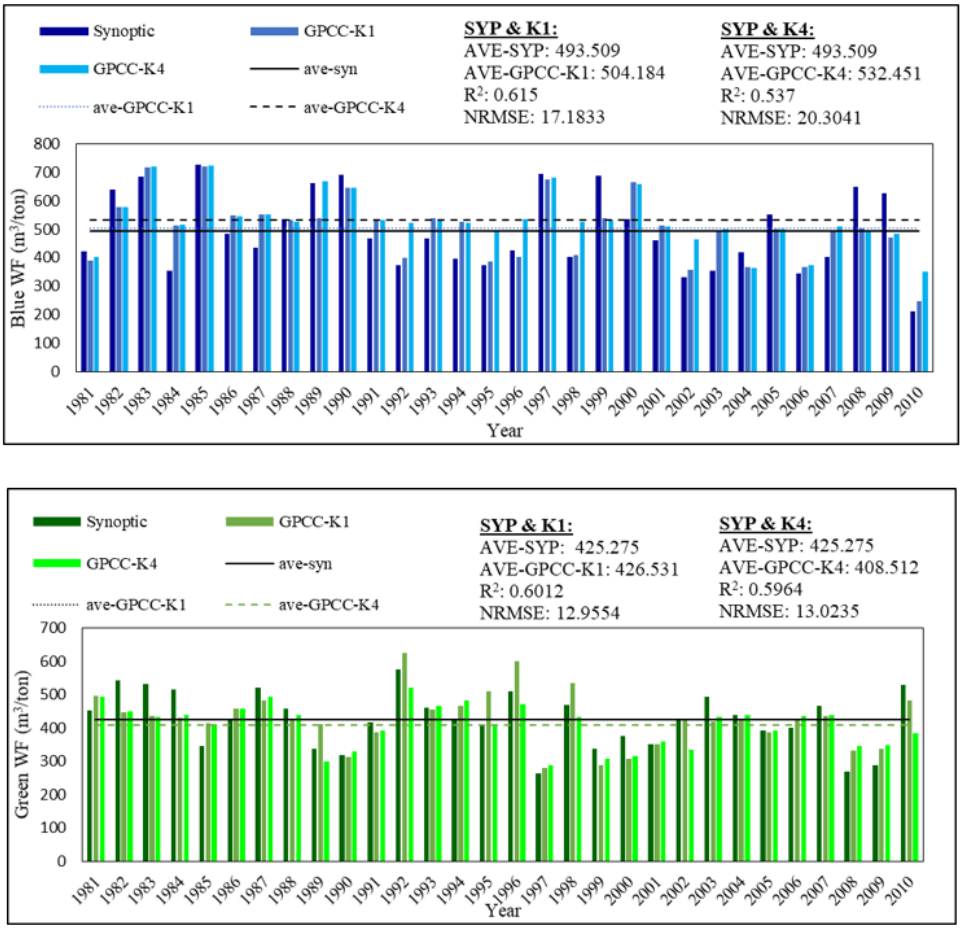

Figure 4. The amounts of blue and green WF of wheat estimated by the synoptic station and GPCC. Ave = Average, SYP = Synoptic Station, K1 = Nearest Neighbor Point, K4 = Four Nearest Neighbor Points.

3.1.3. AgCFSR

The blue and the green WF estimated by the synoptic station and AgCFSR (K1 and K4) are shown

in Figure 5. For the blue WF, the values of R2 for K1 and K4 by AgCFSR are 0.42 and 0.39 with 233.35 and 183 m^3/ton RMSE and 42.28 and 37.08% NRMSE. Also, the amounts of ME for both K1 and K4 are 420.82 and 371.8 m^3/ton, respectively. According to the second figure, the values of R^2 in estimating the K1 and K4 green WF are 0.345 and 0.484. The amounts of RMSE, NRMSE and ME for both K1 and K4 are 143.27 and 137.22 m^3/ton, 33.69 and 32.27%, and 264.42 and 213.74 m^3/ton, respectively. Although K4 is more efficient than K1, AgCFSR is underestimating the blue and the green WF significantly.

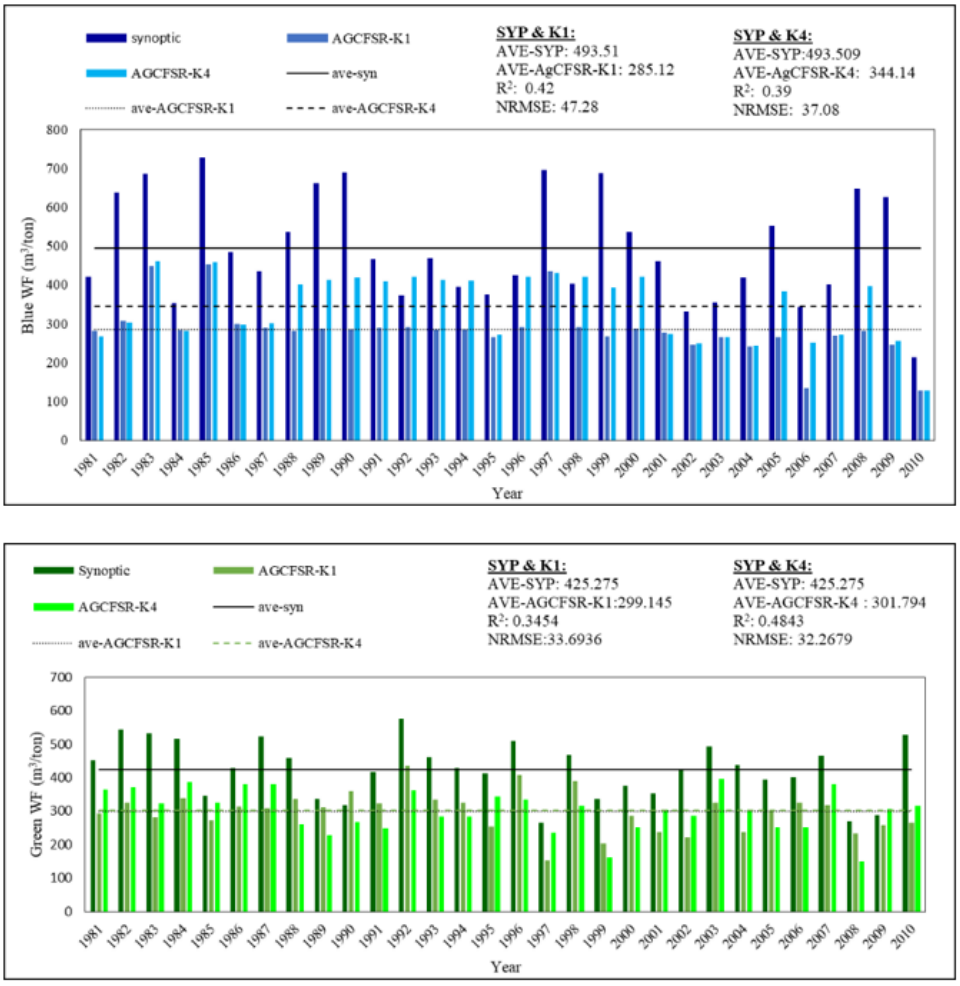

Figure 5. The amounts of the blue and green WF of wheat estimated by the synoptic station and AgCFSR. Ave = Average, SYP = Synoptic Station, K1 = Nearest Neighbor Point, K4 = Four Nearest Neighbor Points.

3.1.4. AgMERRA

In Figure 6, the blue and the green WF estimations of the synoptic station and K1 and K4 of the AgMERRA dataset are represented. According to the blue WF figure, the values of R^2 and RMSE are 0.326 and 189.66 for K1, and 0.275 and 186.43 m^3/ton for K4. For both estimations, the amounts of NRMSE and ME are 38.43 and 37.78% (K1), and 402.66 and 409.52 m^3/ton (K4). The same estimation

of the green WF had R^2 values of 0.253 and 0.31 for K1 and K4, respectively. The amounts of RMSE and NRMSE for K1 and K4 are 145.23 and 128.02 m^3/ton, and 34.15 and 30.1%, respectively. The maximum error of these estimations is 243.6 m^3/ton for the nearest neighbor point (K1) and 220.78 m^3/ton for the four nearest neighbor points (K4). According to the results, K4 in evaluating WF components by AgMERRA is more efficient than the nearest neighbor point. Also, AgMERRA is similar to the AgCFSR dataset in underestimating the blue and the green WF.

Overall, according to the results, all datasets are more efficient in estimating the green WF than the blue WF. Both the nearest neighbor point and the four nearest neighbor points are close to each other. GPCC is the best dataset among these four datasets in estimating the WF components, with less than 26.55 m^3/ton RMSE for the blue WF and 21.3 m^3/ton for the green WF. CRU is the second best dataset, with around 131.03 m^3/ton RMSE for the blue WF and 90.59 m^3/ton RMSE for the green WF. Both AgMERRA and AgCFSR are close in estimating the blue and the green WF.

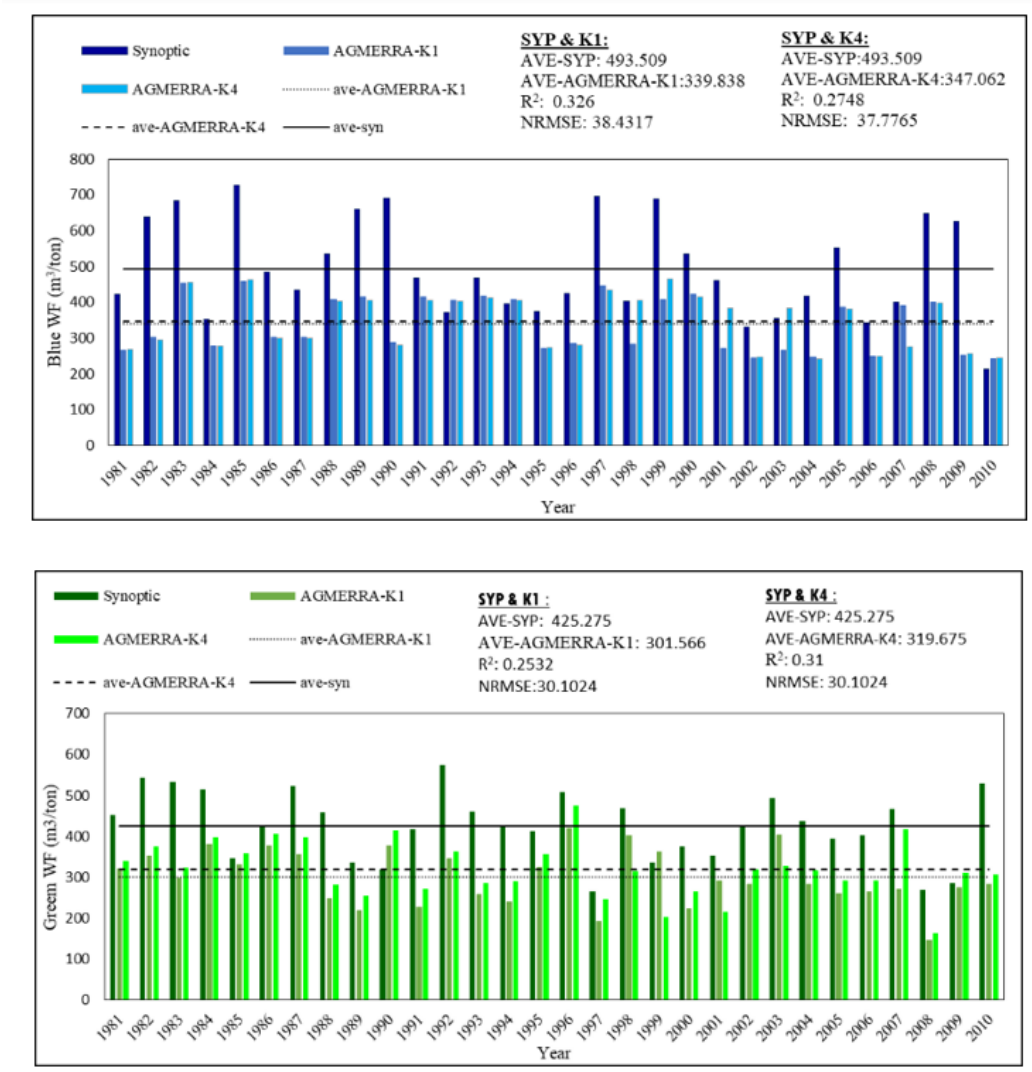

Figure 6. The amounts of blue and green WF of wheat estimated by the synoptic station and AgMERRA. Ave = Average, SYP = Synoptic Station, K1 = Nearest Neighbor Point, K4 = Four Nearest Neighbor Points.

3.2. Maize WF

3.2.1. CRU

In Figure 7, the amounts of the blue and the green WF of maize estimated by the nearest (K1) and the four nearest neighbor points (K4) of CRU are shown against the synoptic station. Although R^2 in all estimations is less than 0.01, other statistic indexes are good, for example, the amounts of RMSE of K1 and K4 are 38.58 and 39.46 m^3/ton for the blue WF, while the NRMSE values are 15.9 and 16.27%, respectively. Meanwhile, 79.8 m^3/ton and 85.21 m^3/ton are the values of maximum error for these two components. On the other hand, the amounts of RMSE and NRMSE for the green WF are 20.53 m^3/ton and 13.74% for K1 estimation and 20.98 m^3/ton and 14.03% for the K4 estimation. The amounts of maximum error in both components are 49.29 m^3/ton and 49.98 m^3/ton. As can be seen, both K1 and K4 estimations of the CRU dataset are close together, while the green WF estimation is more efficient than the blue WF. CRU is underestimating the blue and the green WF of maize for both K1 and K4.

Figure 7. The amounts of the blue and green WF of maize estimated by the synoptic station and CRU. Ave = Average, SYP = Synoptic Station, K1 = Nearest Neighbor Point, K4 = Four Nearest Neighbor Points.

3.2.2. GPCC

The amounts of the blue and the green WF of maize estimated by GPCC (K1 and K4) are represented in Figure 8 against synoptic station. The value of R^2 is less than 0.05 in these datasets, except for the blue WF with K1, which is 0.16. However, the amount of RMSE and NRMSE of the blue WF estimation for K1 and the K4 are 43.07 m^3/ton and 17.75% and 47.75 m^3/ton and 19.66%, respectively. These amounts for the green WF are 18.22 m^3/ton and 12.19% and 17.01 m^3/ton and 11.38%, respectively. The amounts of maximum error for estimating the blue WF are 101.54 and 93.58 m^3/ton for K1 and K4, while they are 47.05 m^3/ton and 34.35 m^3/ton for the green WF, respectively. As can be seen, GPCC is underestimating the amount of blue WF of maize, but the green WF estimations are close to the synoptic station in the province.

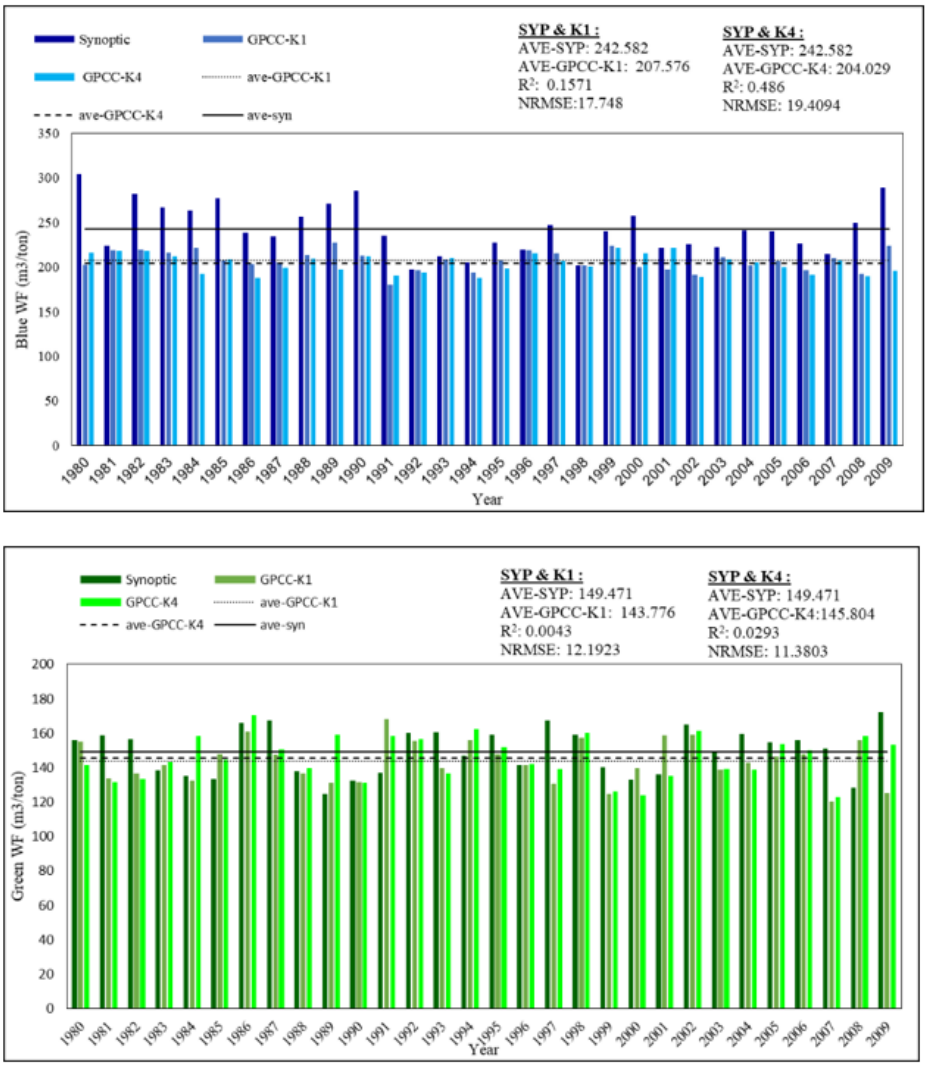

Figure 8. The amounts of the blue and green WF of maize estimated by the synoptic station and GPCC. Ave = Average, SYP = Synoptic Station, K1 = Nearest Neighbor Point, K4 = Four Nearest Neighbor Points.

3.2.3. AgCFSR

In Figure 9, the amounts of the blue WF and the green WF estimated by the synoptic station are shown with the K1 and the K4 of AGCFSR estimation. According to the results, R^2, RMSE, NRMSE and ME for K1 of the blue WF are < 0.01, 39.72 m^3/ton, 16.37% and 82.72 m^3/ton. These amounts are 0.01, 104.98 m^3/ton, 43.27% and 155.44 m^3/ton for K4. On the other hand, the green WF estimations are less than 0.001, 120.31 m^3/ton, 80.49% and 167.05 m^3/ton for K1 and less than 0.001, 40.95 m^3/ton, 40.28%, and 77.78 m^3/ton for K4, respectively. Results show that for this dataset, K1 is more efficient in estimating the blue WF, while K4 is more reliable in estimating the green WF. Here, both blue and green WF are underestimated by the AgCFSR dataset, and the numbers of estimations are different significantly for K1 and K4.

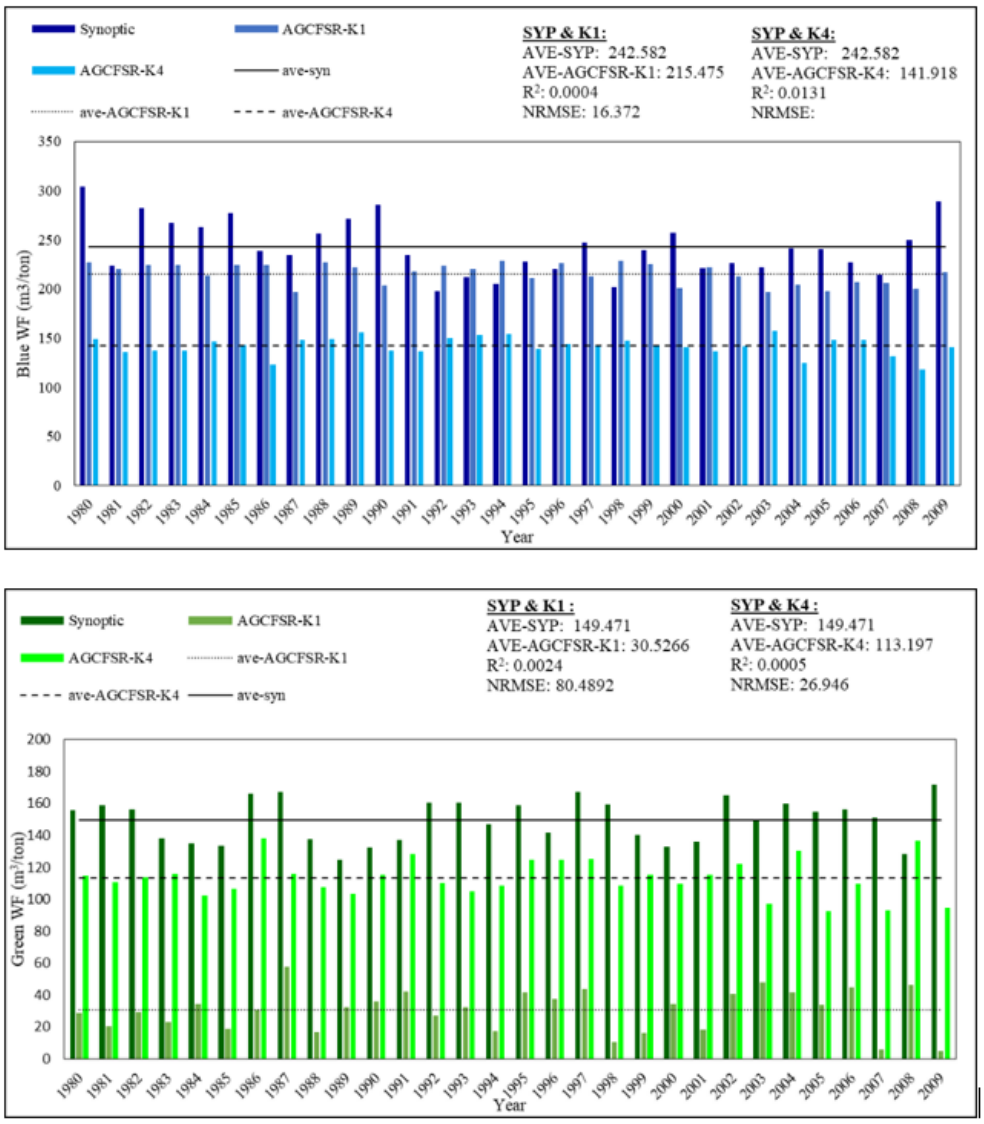

Figure 9. The amounts of the blue and green WF of maize estimated by the synoptic station and AgCFSR. Ave = Average, SYP = Synoptic Station, K1 = Nearest Neighbor Point, K4 = Four Nearest Neighbor Points.

3.2.4. AgMERRA

Finally, in Figure 10, the blue and the green WF are estimated by the synoptic station and K1 and K4 of AgMERRA. The values of R^2 are 0.094 and 0.18 for the blue WF but less than 0.03 for the green WF for both K1 and K4. RMSE and NRMSE for the blue WF are 98.81 and 103.56 m^3/ton and 40.73 and 42.69%, for K1 and K4. The same amounts for the green WF are 42.19 m^3/ton and 28.22% and 36.26 m^3/ton and 24.26%, for K1 and K4. The maximum error of the blue WF is about 160 m^3/ton, while it is around 68 m^3/ton for the green WF. AgMERRA is underestimating the blue and the green WF of maize, but both K1 and K4 estimations are close to each other.

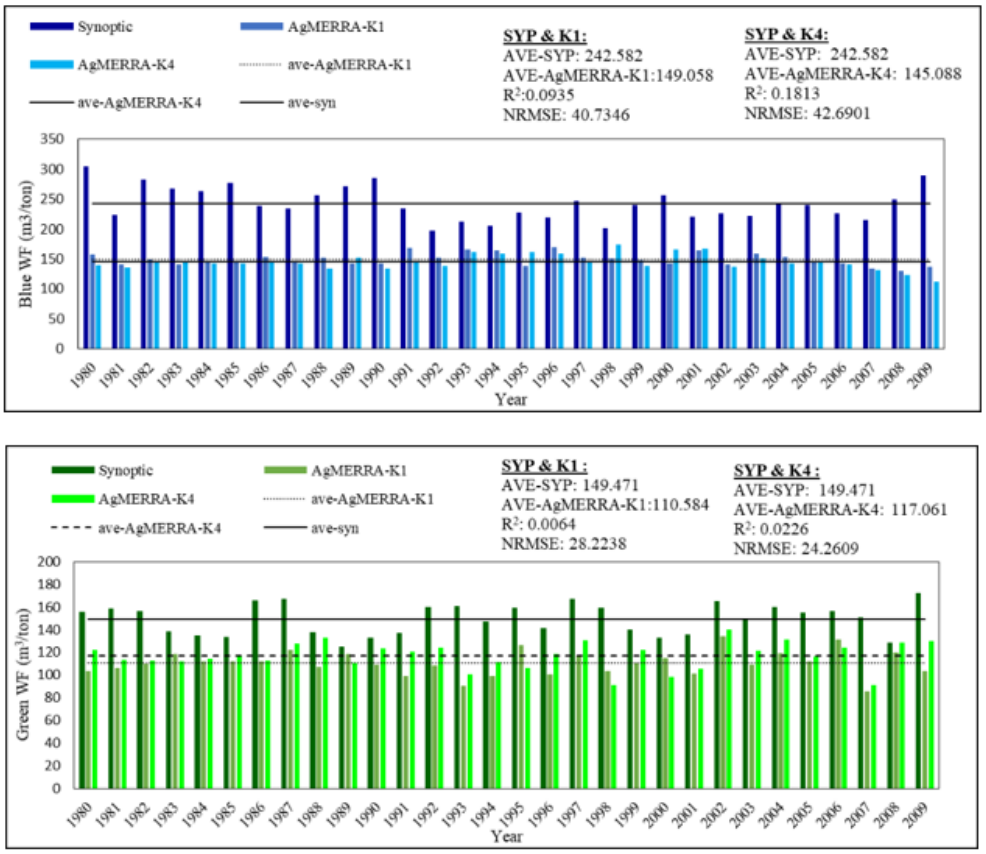

Figure 10. The amounts of the blue and green WF of maize estimated by the synoptic station and AgMERRA. Ave = Average, SYP = Synoptic Station, K1 = Nearest Neighbor Point, K4 = Four Nearest Neighbor Points.

According to analysis and the results, R2 for all datasets are very low and close to zero, but the amounts of other parameters are relatively efficient. In most datasets, estimating the green WF is more efficient than estimating the blue WF. Also, there is no significant difference between K1 and K4 in estimating the WF components by CRU and GPCC datasets, while in the other two datasets, K1 is more efficient. Overall, in estimating the WF components, CRU is the most efficient, and GPCC, with a slight difference, is the second-most efficient dataset in this study.

4. Discussion

According to the results, CRU and GPCC were the most efficient datasets among four understudy datasets, and they can be used in managerial studies and research. In a study that gridded precipitation datasets evaluated over arid regions, GPCC was more efficient than CRU [71]. Similar results were reported by another study related to statistical tests of APHRODITE and GPCC [81]. One of the main reasons for GPCC having higher efficiency than CRU is the number of weather stations, which is 85000 against 4000, respectively [74]. In another study, the production and water requirement of wheat was estimated based on some meteorological datasets and then compared with the synoptic station. It was found out that they reached similar results for CRU, AgMERRA and AgCFSR. They also claimed the highest accuracy of GPCC-CR for water requirement estimations and AgMERRA for wheat production estimations [82].

On the other hand, there have been numerous studies relating to using meteorological datasets in climate and crop factors. Most of them were similar in suggesting the use of these datasets in agricultural and water resources management. They claimed the importance of using these datasets instead of synoptic stations and classical measurements, such as Ababaei and Ramezani (2021) that used CRU for a 60-year period [83]. Also, Shi et al. (2017) evaluated the CRU TS precipitation dataset for the Three-River Headwaters Region. The results showed that CRU underestimates the annual precipitation compared to point rain gauge records data. They also claimed the importance of using a gridded precipitation dataset to have a clearer understating of the spatio-temporal patterns of precipitation in high-elevation mountainous regions where ground precipitation measurements are not widely available [28]. Salvacion et al. (2018) used raw and downscaled CRU data to estimate precipitation in the Philippines. They showed that the raw CRU dataset underestimates precipitation for most of the month in the study, while the downscaled CRU tends to overestimate. According to the result, the downscaled CRU performed better with higher accuracy [84]. The CRU dataset was also applied for Iran over a 60-year period to estimate crop water requirement and showed high performance [85].

Ababaei (2020) used CRU and GPCC to investigate temporal trends of seven climatic variables and their spatial distributions across Iran. He deduced these two datasets are promising alternatives to weather station observations [86]. Zhu et al. (2015) investigated the reliability of four datasets (CRU TS, GPCC, Delware and NOAA) with resolution of 0.5°×0.5° in Xinjiang. They showed that all datasets were able to simulate the main spatial pattern and seasonal variation of precipitation [87].

After version 4 of the CRU dataset, the accuracy of this dataset was demonstrated in many studies for monthly climate variables as well. This dataset covers almost all the lands on Earth (except Antarctica) with high climatology data for both accessible synoptic stations and disadvantaged regions [72].

Lashkari et al. (2018) used AgMERRA to estimate the maximum temperature at the Mashhad station. The R^2 coefficient of this dataset for two different stations in the province was 0.25 and 0.43. They showed that this dataset is reliable in estimating missing data of temperature. Also, this dataset's performance in estimating daily precipitation was efficient, though the distribution of the estimated precipitation was not the same as the observation precipitation [88]. Yaghoubi et al. (2020) evaluated AgMERRA performance to estimate evapotranspiration and yield rainfed wheat in northeast Iran. The highest correlation between the estimated amounts and the observations was 0.7. Also, the amount of NRMSE between climate variables was less than 30%, except for daily wind speed and precipitation at all locations. They concluded that AgMERRA could estimate average ETc and wheat yield in the

long term efficiently, but it is not as efficient for short-term calculations [89]. Salehnia et al. (2017) used AgMERRA to estimate meteorological drought indices, then evaluate it with station-observed precipitation data. They showed that this dataset is efficient in filling gaps in station-observed precipitation data. Also, by station-observed testing, it can be useful in data-lacking areas for estimating precipitation [90].

Although CRU was more efficient in estimating the WF components in this study, Ahmadi et al. (2020) showed that AgMERRA and AgCFSR datasets are more accurate in estimating the minimum and the maximum temperatures than CRU [91]. According to another study, how these datasets are configured and how observational data are analyzed in the specific region may change the outputs [92]. Ruane et al. (2015) used AgMERRA and AgCFSR in agricultural modeling and showed the high accuracy of these two datasets in historical observation and future climate scenarios [93].

There have been other studies that focused on other datasets. For instance, Faraji et al. (2017) used GLDAS data to estimate evapotranspiration precipitation, and air temperature of the Qazvin province. They showed that R^2 for air and soil temperature, potential precipitation and evaporation of this model was 0.9, 0.7 and 0.8 for the Qazvin province. Also, the GLDAS model was not efficient in estimating the amount of flood runoff [94]. Blankenau et al. (2020) evaluated six gridded weather datasets (GLDAS-1, NLDAS-2, CFSv2, GridMet, RTMA and NDFD) with 103 weather stations in well-watered settings all over the United States. Results showed that RTMA was the best gridded data for all variables, while NLDAS was the least efficient except vapor pressure [95]. Another study related to estimating the evapotranspiration by the GLDAS dataset showed high coefficient with acceptable RMSE [96].

5. Conclusions

In this study, thirty-year data from four meteorological datasets were used to estimate the WF components of two main crops in the Qazvin province, wheat and maize. Although the different datasets are developed for different purposes, we wanted to see if we can take advantage of using them for other purposes, which here was to estimate the water footprint of agricultural crops for a managing purpose. Estimates were evaluated by the synoptic stations in the province. The nearest neighbor point and the four nearest neighbor points were used to estimate the WF components.

The steps of this study are given as below:

1. Thirty-year data from four different meteorological datasets was gathered by the nearest (K1) and the average of four nearest neighbor points (K4) to the synoptic station in the Qazvin province;
2. Thirty-year data from the synoptic station was gathered;
3. The AquaCrop model was used to calculate WF based on the gathered data;
4. The WF components were calculated for both datasets and the synoptic station;
5. Results were compared with each other.

Results showed that most datasets are more efficient in estimating the green WF rather than the blue WF. Both the nearest neighbor point and the four nearest neighbor points were close to each other, though the K1 estimations were more efficient in most cases. For estimating the blue WF of wheat, GPCC was more efficient among these four datasets. CRU and AgMERRA were the second and third efficient datasets, while AgCFSR was the least efficient dataset among these four. On the other hand, CRU was more efficient in estimating the green WF components. The values of RMSE and NRMSE for green WF estimated by the GPCC dataset were more efficient, while the blue WF estimated by this

dataset was not as efficient as these amounts. AgCFSR and AgMERRA are the other two datasets with less efficient estimations. According to the results, the datasets were more efficient in estimating maize WF components than wheat. This study shows and suggests using different datasets in estimating WF components for various crops in different regions for irrigation and agricultural management. Also, it needs to be mentioned that the application of these datasets might have some limitations. For example, they might not be able to capture short term weather variations or small regions in their spatial resolution. On the other hand, they might have some bias in sparse observation networks. Data must be localized to have more accurate results and be generalized for the local conditions.

In the future, researchers might be interested in applying these datasets to other regions with different climate or different agricultural products. They also have the opportunity to compare our results with other datasets for the same location. Moreover, they can use these datasets for the regions with no observational data and try to assess the accuracy of datasets with future measured data.

Use of AI tools declaration

The authors declare they have not used artificial intelligence (AI) tools in the creation of this article.

Acknowledgments

The authors would like to express their highly gratitude of four available and free datasets for providing data that were used in this study (CRU TS, GPCC, AgMERRA, and AgCFSR).

Conflict of interest

The authors declare no conflict of interest.

References

1. Massah Bavani A, Morid S (2006) Assessment Aquacrop Model to predict the sugarcane yield and soil salinity profiles under salinity stress. *J Sci Technol Agric Nat Resour* 9: 273–290.
2. del Refugio Barba-López M, Filonov A, Alcocer J, et al. (2021) Complex interactions between meteorological parameters and the thermal regime of two tropical, high altitude crater lakes (Nevado de Toluca, Mexico). *Sci Total Environ* 771: 145310. https://doi.org/10.1016/j.scitotenv.2021.145310
3. Elbeltagi A, Deng J, Wang K, et al. (2020) Modeling long-term dynamics of crop evapotranspiration using deep learning in a semi-arid environment. *Agric Water Manag* 241: 106334. https://doi.org/10.1016/j.agwat.2020.106334
4. Elbeltagi A, Rizwan M, Malik A, et al. (2020) The impact of climate changes on the water footprint of wheat and maize production in the Nile Delta, Egypt. *Sci Total Environ* 743: 140770. https://doi.org/10.1016/j.scitotenv.2020.140770
5. Elbeltagi A, Deng J, Wang K, et al. (2020) Crop water footprint estimation and modeling using an artificial neural network approach in the Nile Delta, Egypt. *Agric Water Manag* 235: 106080. https://doi.org/10.1016/j.agwat.2020.106080

6. Worqlul AW, Collick AS, Tilahun SA, et al. (2015) Comparing TRMM 3B42, CFSR and ground-based rainfall estimates as input for hydrological models, in data scarce regions: the Upper Blue Nile Basin, Ethiopia. *Hydrol Earth Syst Sci Discuss* 12: 2081–2112. https://doi.org/10.5194/hessd-12-2081-2015
7. Hoque MAA, Pradhan B, Ahmed N, et al. (2021) Agricultural drought risk assessment of Northern New South Wales, Australia using geospatial techniques. *Sci Total Environ* 756: 143600. https://doi.org/10.1016/j.scitotenv.2020.143600
8. Fathololoumi S, Vaezi AR, Alavipanah SK, et al. (2020) Comparison of spectral and spatial-based approaches for mapping the local variation of soil moisture in a semi-arid mountainous area. *Sci Total Environ* 724: 138319. https://doi.org/10.1016/j.scitotenv.2020.138319
9. Steiner M, Bell TL, Zhang Y, et al. (2003) Comparison of two methods for estimating the sampling-related uncertainty of satellite rainfall averages based on a large radar dataset. *J Clim* 16: 3759–3778. https://doi.org/10.1175/1520-0442(2003)016%3C3759:COTMFE%3E2.0.CO;2
10. Dixit PN, Telleria R (2015) Advancing the climate data driven crop-modeling studies in the dry areas of Northern Syria and Lebanon: An important first step for assessing impact of future climate. *Sci Total Environ* 511: 562–575. https://doi.org/10.1016/j.scitotenv.2015.01.001
11. Kheirinejad S, Bozorg-Haddad O, Singh VP, et al. (2022) The effect of reducing per capita water and energy uses on renewable water resources in the water, food and energy nexus. *Sci Rep* 12: 7582. https://doi.org/10.1038/s41598-022-11595-w
12. Ghorbany S, Noorzai E, Yousefi S (2023) BIM-based solution to enhance the performance of public-private partnership construction projects using copula bayesian network. *Expert Syst Appl* 216: 119501. https://doi.org/10.1016/j.eswa.2023.119501
13. Ghorbany S, Yousefi S, Noorzai E (2022) Evaluating and optimizing performance of public–private partnership projects using copula Bayesian network. *Eng Constr Archit Manag* ahead-of-print. https://doi.org/10.2139/ssrn.4012554
14. Jones JW, Hoogenboom G, Porter CH, et al. (2003) The DSSAT cropping system model. *Eur J Agron* 18: 235–265. https://doi.org/10.1016/S1161-0301(02)00107-7
15. Stöckle CO, Donatelli M, Nelson R (2003) CropSyst, a cropping systems simulation model. *Eur J Agron* 18: 289–307. https://doi.org/10.1016/S1161-0301(02)00109-0
16. Keating BA, Carberry PS, Hammer GL, et al. (2003) An overview of APSIM, a model designed for farming systems simulation. *Eur J Agron* 18: 267–288. https://doi.org/10.1016/S1161-0301(02)00108-9
17. Yang HS, Dobermann A, Lindquist JL, et al. (2004) Hybrid-maize—A maize simulation model that combines two crop modeling approaches. *F Crop Res* 87: 131–154. https://doi.org/10.1016/j.fcr.2003.10.003
18. El-mageed A, Ibrahim MM, Elbeltagi AM (2017) The effect of water stress on nitrogen status as well as water use efficiency of potato crop under drip irrigation system. *Misr J Ag Eng* 34: 1351–1374. https://doi.org/10.21608/mjae.2017.97473
19. Queyrel W, Habets F, Blanchoud H, et al. (2016) Pesticide fate modeling in soils with the crop model STICS: Feasibility for assessment of agricultural practices. *Sci Total Environ* 542: 787–802. https://doi.org/10.1016/j.scitotenv.2015.10.066
20. Raes D, Steduto P, Hsiao TC, et al. (2009) Aquacrop—The FAO crop model to simulate yield response to water: II. main algorithms and software description. *Agron J* 101: 438–447. https://doi.org/10.2134/agronj2008.0140s

21. Steduto P, Hsiao TC, Raes D, et al. (2009) AquaCrop—The FAO Crop Model to Simulate Yield Response to Water: I. Concepts and Underlying Principles. *Agron J* 101: 426–437. https://doi.org/10.2134/agronj2008.0139s
22. Ahmad M (2013) Simulation of wheat yield by AquaCrop model. *Int J Farm Allied Sci* 2: 939–943.
23. Abedinpour M, Sarangi A, Rajput TBS, et al. (2012) Performance evaluation of AquaCrop model for maize crop in a semi-arid environment. *Agric Water Manag* 110: 55–66. https://doi.org/10.1016/j.agwat.2012.04.001
24. Hellal F, Mansour H, Abdel-Hady M, et al. (2019) Assessment water productivity of barley varieties under water stress by AquaCrop model. *AIMS Agric Food* 4: 501–517. https://doi.org/10.3934/agrfood.2019.3.501
25. García-Vila M, Fereres E, Mateos L, et al. (2009) Defi cit irrigation optimization of cotton with aquacrop. *Agron J* 101: 477–487. https://doi.org/10.2134/agronj2008.0179s
26. Gobin A, Kersebaum K, Eitzinger J, et al. (2017) Variability in the water footprint of arable crop production across European regions. *Water* 9: 93. https://doi.org/10.3390/w9020093
27. Ramezani Etedali H, Adabi V, Gorgin F, et al. (2023) The probabilistic behavior of AquaCrop parameters: A Monte-Carlo study. *Stoch Environ Res Risk Assess* 37: 717–734. https://doi.org/10.1007/s00477-022-02309-9
28. Shi H, Li T, Wei J (2017) Evaluation of the gridded CRU TS precipitation dataset with the point raingauge records over the Three-River Headwaters Region. *J Hydrol* 548: 322–332. https://doi.org/10.1016/j.jhydrol.2017.03.017
29. Ge Y, Zhang K, Yang X (2019) A 110-year pollen record of land use and land cover changes in an anthropogenic watershed landscape, eastern China: Understanding past human-environment interactions. *Sci Total Environ* 650: 2906–2918. https://doi.org/10.1016/j.scitotenv.2018.10.058
30. Rodriguez J, Ustin S, Sandoval-Solis S, et al. (2015) Food, water, and fault lines: Remote sensing opportunities for earthquake-response management of agricultural water. *Sci Total Environ* 565: 1020–1027. https://doi.org/10.1016/j.scitotenv.2016.05.146
31. Ollivier C, Olioso A, Carrière SD, et al. (2021) An evapotranspiration model driven by remote sensing data for assessing groundwater resource in karst watershed. *Sci Total Environ* 781: 146706. https://doi.org/10.1016/j.scitotenv.2021.146706
32. Capolongo D, Refice A, Bocchiola D, et al. (2019) Coupling multitemporal remote sensing with geomorphology and hydrological modeling for post flood recovery in the Strymonas dammed river basin (Greece). *Sci Total Environ* 651: 1958–1968. https://doi.org/10.1016/j.scitotenv.2018.10.114
33. Javed T, Li Y, Rashid S, et al. (2021) Performance and relationship of four different agricultural drought indices for drought monitoring in China's mainland using remote sensing data. *Sci Total Environ* 759: 143530. https://doi.org/10.1016/j.scitotenv.2020.143530
34. Vulova S, Meier F, Rocha AD, et al. (2021) Modeling urban evapotranspiration using remote sensing, flux footprints, and artificial intelligence. *Sci Total Environ* 786: 147293. https://doi.org/10.1016/j.scitotenv.2021.147293
35. Li J, Tian L, Wang Y, et al. (2021) Optimal sampling strategy of water quality monitoring at high dynamic lakes: A remote sensing and spatial simulated annealing integrated approach. *Sci Total Environ* 777: 146113. https://doi.org/10.1016/j.scitotenv.2021.146113
36. Vadrevu KP, Badarinath KVS, Eaturu A (2008) Spatio-temporal analysis of fire events in India: Implications for environmental conservation. *J Environ Plan Manag* 51: 817–832. https://doi.org/10.1080/09640560802423657

37. Apan AA, Raine SR, Le Brocque A, et al. (2004) Spatial prioritization of revegetation sites for dryland salinity management: An analytical framework using GIS. *J Environ Plan Manag* 47: 811–825. https://doi.org/10.1080/0964056042000284848
38. Olivera Rodriguez P, Holzman ME, Degano MF, et al. (2021) Spatial variability of the green water footprint using a medium-resolution remote sensing technique: The case of soybean production in the Southeast Argentine Pampas. *Sci Total Environ* 763: 142963. https://doi.org/10.1016/j.scitotenv.2020.142963
39. Yang H, Wang L, Abbaspour KC, et al. (2006) Virtual water trade: An assessment of water use efficiency in the international food trade. *Hydrol Earth Syst Sci* 10: 443–454. https://doi.org/10.5194/hess-10-443-2006
40. Hoekstra AY (2003) Virtual water: An introduction. *Virtual Water Trade* 13: 108.
41. Chapagain AK, Hoekstra AY (2011) The blue, green and grey water footprint of rice from production and consumption perspectives. *Ecol Econ* 70: 749–758. https://doi.org/10.1201/b10541-17
42. Zoumides C, Bruggeman A, Hadjikakou M, et al. (2014) Policy-relevant indicators for semi-arid nations: The water footprint of crop production and supply utilization of Cyprus. *Ecol Indic* 43: 205–214. https://doi.org/10.1016/j.ecolind.2014.02.012
43. Bazrafshan O, Zamani H, Ramezanietedli H, et al. (2020) Improving water management in date palms using economic value of water footprint and virtual water trade concepts in Iran. *Agric Water Manag* 229: 105941. https://doi.org/10.1016/j.agwat.2019.105941
44. Qasemipour E, Abbasi A (2019) Virtual water flow and water footprint assessment of an arid region: A case study of South Khorasan Province, Iran. *Water* 11: 1755. https://doi.org/10.3390/w11091755
45. Qasemipour E, Tarahomi F, Pahlow M, et al. (2020) Assessment of virtual water flows in Iran using a multi-regional input-output analysis. *Sustainability* 12: 7424. https://doi.org/10.3390/su12187424
46. Ababaei B, Ramezani Etedali H (2014) Estimation of water footprint components of Iran's wheat production: Comparison of global and national scale estimates. *Environ Process* 1: 193–205. https://doi.org/10.1007/s40710-014-0017-7
47. Ababaei B, Ramezani Etedali H (2017) Water footprint assessment of main cereals in Iran. *Agric Water Manag* 179: 401–411. https://doi.org/10.1016/j.agwat.2016.07.016
48. Zhuo L, Hoekstra AY, Wu P, et al. (2019) Monthly blue water footprint caps in a river basin to achieve sustainable water consumption: The role of reservoirs. *Sci Total Environ* 650: 891–899. https://doi.org/10.1016/j.scitotenv.2018.09.090
49. Li E, Li S, Endter-Wada J (2017) Water-smart growth planning: linking water and land in the arid urbanizing American West. *J Environ Plan Manag* 60: 1056–1072. https://doi.org/10.1080/09640568.2016.1197106
50. Serio F, Miglietta PP, Lamastra L, et al. (2018) Groundwater nitrate contamination and agricultural land use: A grey water footprint perspective in Southern Apulia Region (Italy). *Sci Total Environ* 645: 1425–1431. https://doi.org/10.1016/j.scitotenv.2018.07.241
51. Mojtabavi SA, Shokoohi A, Ramezani Etedali H, et al. (2018) Using regional virtual water trade and water footprint accounting for optimizing crop patterns to mitigate water crises in dry regions. *Irrig Drain* 67: 295–305. https://doi.org/10.1002/ird.2170
52. Ramezani Etedali H, Ahmadaali K, Gorgin F, et al. (2019) Optimization of the cropping pattern of main cereals and improving water productivity: application of the water footprint concept. *Irrig Drain* 68: 765–777. https://doi.org/10.1002/ird.2362

53. Nazari R, Ramezani Etedali H, Nazari B, et al. (2020) The impact of climate variability on water footprint components of rainfed wheat and barley in the Qazvin province of Iran. *Irrig Drain* 69: 826–843. https://doi.org/10.1002/ird.2487
54. Grammatikopoulou I, Sylla M, Zoumides C (2020) Economic evaluation of green water in cereal crop production: A production function approach. *Water Resour Econ* 29: 100148. https://doi.org/10.1016/j.wre.2019.100148
55. Cui S, Zhang J, Wang X, et al. (2023) Fuzzy composite risk assessment of water-energy-food-carbon nexus in the dispark pumped irrigation system. *J Hydrol* 624: 129879. https://doi.org/10.1016/j.jhydrol.2023.129879
56. Cao X, Zeng W, Wu M, et al. (2020) Hybrid analytical framework for regional agricultural water resource utilization and efficiency evaluation. *Agric Water Manag* 231: 106027. https://doi.org/10.1016/j.agwat.2020.106027
57. Cao X, Wu N, Adamowski J, et al. (2023) Assessing the contribution of China's grain production during 2005–2020 from the perspective of the crop-water-land nexus. *J Hydrol* 626: 130376. https://doi.org/10.1016/j.jhydrol.2023.130376
58. Kakvand P, Ramezani Etedali H, Gorgin Paveh F (2020) *Estimation of Maize Water Footprint Based on GPCC and AgCFSR Gridded Datasets*. IV International Eurasian Agriculture and Natural Sciences Congress.
59. Gorgin Paveh F, Ramezani Etedali H, Collins B (2022) Evaluation of CRU TS, GPCC, AgMERRA, and AgCFSR meteorological datasets for estimating climate and crop variables: A case study of maize in Qazvin Province, Iran. *J Arid Land* 14: 1361–1376. https://doi.org/10.1007/s40333-022-0108-7
60. GorginPaveh F, Ramezani Etedali H, Kakvand P (2020) *Estimation of Wheat Water footprint Based on CRU and AgMERRA Gridded Datasets*. IV International Eurasian Agriculture and Natural Sciences Congress.
61. Mohammadrezapour O, Yoosefdoost I, Ebrahimi M (2019) Cuckoo optimization algorithm in optimal water allocation and crop planning under various weather conditions (case study: Qazvin plain, Iran). *Neural Comput Appl* 31: 1879–1892.
62. Chapagain AK, Hoekstra AY (2008) The global component of freshwater demand and supply: An assessment of virtual water flows between nations as a result of trade in agricultural and industrial products. *Water Int* 33: 19–32. https://doi.org/10.1080/02508060801927812
63. Hoekstra A, Chapagain A, Aldaya M, et al. (2009) *Water footprint manual.* Ambio.
64. Chapagain AK (2017) Water footprint: State of the art: What, why, and how? In: Abraham MA (Eds.), *Encyclopedia of Sustainable Technologies,* Elsevier, 153–163. https://doi.org/10.1016/B978-0-12-409548-9.10164-2
65. Muthu SS (2020) 4—Calculating the water and energy footprints of textile products. *Assessing the Environmental Impact of Textiles and the Clothing Supply Chain,* Elsevier, 77–93. https://doi.org/10.1016/B978-0-12-819783-7.00004-1
66. Merrett S, Allan JA, Lant C (2003) Virtual water—The water, food, and trade nexus useful concept or misleading metaphor? *Water Int* 28: 106–113. https://doi.org/10.1080/02508060.2003.9724812
67. Allen RG, Pereira LS, Raes D, et al. (1998) Crop evapotranspiration: Guidelines for computing crop requirements. Irrig Drain Pap No 56, FAO.
68. Rahimikhoob H, Sotoodehnia A, Massahbavani AR (2014) Calibration and evaluation of AquaCrop for maize in Qazvin region. *Iran J Irrig Drain* 8: 108–115.

69. Chen YR, Chu PS (2014) Trends in precipitation extremes and return levels in the Hawaiian Islands under a changing climate. *Int J Climatol* 34: 3913–3925. https://doi.org/10.1002/joc.3950
70. Khalili A, Rahimi J (2014) High-resolution spatiotemporal distribution of precipitation in Iran: A comparative study with three global-precipitation datasets. *Theor Appl Climatol* 118: 211–221. https://doi.org/10.1007/s00704-013-1055-1
71. Ahmed K, Shahid S, Wang X, et al. (2019) Evaluation of gridded precipitation datasets over arid regions of Pakistan. *Water (Switzerland)* 11: 210. https://doi.org/10.3390/w11020210
72. Harris I, Osborn TJ, Jones P, et al. (2020) Version 4 of the CRU TS monthly high-resolution gridded multivariate climate dataset. *Sci Data* 7: 109. https://doi.org/10.1038/s41597-020-0453-3
73. Mitchell TD, Jones PD (2005) An improved method of constructing a database of monthly climate observations and associated high-resolution grids. *Int J Climatol* 25: 693–712. https://doi.org/10.1002/joc.1181
74. Schneider U, Becker A, Finger P, et al. (2014) GPCC's new land surface precipitation climatology based on quality-controlled in situ data and its role in quantifying the global water cycle. *Theor Appl Climatol* 115: 15–40. https://doi.org/10.1007/s00704-013-0860-x
75. Becker A, Finger P, Meyer-Christoffer A, et al. (2013) A description of the global land-surface precipitation data products of the Global Precipitation Climatology Centre with sample applications including centennial (trend) analysis from 1901-present. *Earth Syst Sci Data* 5: 921–998. https://doi.org/10.5194/essdd-5-921-2012
76. Von Lampe M, Willenbockel D, Ahammad H, et al. (2014) Why do global long-term scenarios for agriculture differ? An overview of the AgMIP global economic model intercomparison. *Agric Econ (United Kingdom)* 45: 3–20. https://doi.org/10.1111/agec.12086
77. Nelson GC, Valin H, Sands RD, et al. (2014) Climate change effects on agriculture: Economic responses to biophysical shocks. *Proc Natl Acad Sci* 111: 3274–3279.
78. Rosenzweig C, Jones JW, Hatfield JL, et al. (2013) The Agricultural Model Intercomparison and Improvement Project (AgMIP): Protocols and pilot studies. *Agric For Meteorol* 170: 166–182. https://doi.org/10.1016/j.agrformet.2012.09.011
79. Doorenbos J, Kassam A. (1979) Yield response to water. In: Doorenbos J, Kassam AH, Bentvelsen C, et al. (Eds.), *Irrigation and Agricultural Development,* Based on an International Expert Consultation, Baghdad, Iraq, 257–280. https://doi.org/10.1016/B978-0-08-025675-7.50021-2
80. Golabi M, Naseri AA (2015) Assessment Aquacrop Model to predict the sugarcane yield and soil salinity profiles under salinity stress. *Iran J Soil Water Res* 4: 685–694.
81. Duethmann D, Zimmer J, Gafurov A, et al. (2013) Evaluation of areal precipitation estimates based on downscaled reanalysis and station data by hydrological modelling. *Hydrol Earth Syst Sci Discuss* 9: 10719–10773. https://doi.org/10.5194/hessd-9-10719-2012
82. Bahroloum R, Ramezani Etedali H, Azizian A, et al. (2020) Use of gridded weather datasets in simulation of wheat yield and water requirement (Case Study: Iran's Qazvin Plain). *Ecohydrology* 7: 691–706.
83. Ababaei B, Ramezanietedli H (2021) Investigating spatiotemporal variations of precipitation across Iran over 1957–2016 using the CRU gridded dataset. *Modares Civ Eng J* 21: 103–117.
84. Salvacion AR, Magcale-Macandog DB, Cruz PCS, et al. (2018) Evaluation and spatial downscaling of CRU TS precipitation data in the Philippines. *Model Earth Syst Environ* 4: 891–898. https://doi.org/10.1007/s40808-018-0477-2

85. Collins B, Ramezani Etedali H, Tavakol A, et al. (2021) Spatiotemporal variations of evapotranspiration and reference crop water requirement over 1957–2016 in Iran based on CRU TS gridded dataset. *J Arid Land* 13: 858–878. https://doi.org/10.1007/s40333-021-0103-4
86. Ababaei B (2020) Spatio—Temporal variations of seven weather variables in Iran: application of CRU TS and GPCC data sets. *Irrig Drain* 69: 164–185. https://doi.org/10.1002/ird.2399
87. Zhu X, Zhang M, Wang S, et al. (2015) Comparison of monthly precipitation derived from high-resolution gridded datasets in arid Xinjiang, central Asia. *Quat Int* 358: 160–170. https://doi.org/10.1016/j.quaint.2014.12.027
88. Lashkari A, Salehnia N, Asadi S, et al. (2018) Evaluation of different gridded rainfall datasets for rainfed wheat yield prediction in an arid environment. *Int J Biometeorol* 62: 1543–1556. https://doi.org/10.1007/s00484-018-1555-x
89. Yaghoubi F, Bannayan M, Asadi GA (2020) Performance of predicted evapotranspiration and yield of rainfed wheat in the northeast Iran using gridded AgMERRA weather data. *Int J Biometeorol* 64: 1519–1537. https://doi.org/10.1007/s00484-020-01931-y
90. Salehnia N, Alizadeh A, Sanaeinejad H, et al. (2017) Estimation of meteorological drought indices based on AgMERRA precipitation data and station-observed precipitation data. *J Arid Land* 9: 797–809. https://doi.org/10.1007/s40333-017-0070-y
91. Ahmadi M, Ramezani Etedali H, Elbeltagi A (2021) Evaluation of the effect of climate change on maize water footprint under RCPs scenarios in Qazvin plain, Iran. *Agric Water Manag* 254: 106969. https://doi.org/10.1016/j.agwat.2021.106969
92. Hajihoseini H, Hajihoseini M, Najafi A, et al. (2015) Assessment of changes in hydro-meteorological variables upstream of Helmand Basin during the last century using CRU data and SWAT model. *Iran Water Resour Res* 10: 38–52.
93. Ruane AC, Goldberg R, Chryssanthacopoulos J (2015) Climate forcing datasets for agricultural modeling: Merged products for gap-filling and historical climate series estimation. *Agric For Meteorol* 200: 233–248. https://doi.org/10.1016/j.agrformet.2014.09.016
94. Faraji Z, Kaviani A, Shakiba A (2017) Evaluation of evapotranspiration, precipitation and air temperature from Global Land Data Assimilation System (GLDAS) by Lysimeter Data in Qazvin. *J Water Soil Conserv* 24: 283–297.
95. Blankenau PA, Kilic A, Allen R (2020) An evaluation of gridded weather data sets for the purpose of estimating reference evapotranspiration in the United States. *Agric Water Manag* 242: 106376. https://doi.org/10.1016/j.agwat.2020.106376
96. Moiwo JP, Yang Y, Li H, et al. (2009) Comparison of GRACE with in situ hydrological measurement data shows storage depletion in Hai River Basin, Northern China. *Water SA* 35: . https://doi.org/10.4314/wsa.v35i5.49192

AIMS Press